CAMBRIDGE
UNIVERSITY PRESS

Article

Arsenoústalečite, $Cu_{12}(As_2Te_2)Se_{13}$, a new mineral, and crystal structures of arsenoústalečite and stibioústalečite

Jiří Sejkora[1] , Cristian Biagioni[2,3] , Pavel Škácha[1,4], Silvia Musetti[2] and Daniela Mauro[2,5]

[1]Department of Mineralogy and Petrology, National Museum, Cirkusová 1740, 193 00, Praha 9, Czech Republic; [2]Dipartimento di Scienze della Terra, Università di Pisa, Via Santa Maria, 53, I-56126 Pisa, Italy; [3]Centro per l'Integrazione della Strumentazione Scientifica dell'Università di Pisa, Università di Pisa, Italy; [4]Mining Museum Příbram, Hynka Kličky Place 293, 261 01 Příbram VI, Czech Republic; and [5]Museo di Storia Naturale, Università di Pisa, Via Roma 79, I-56011 Calci (PI), Italy

Abstract

Arsenoústalečite is a new mineral discovered in a sample collected from the abandoned Ústaleč deposit near Horažďovice, SW Bohemia, Czech Republic. It occurs as rare anhedral grains, up to 40 μm in size, in a calcite gangue, associated with stibioústalečite, hakite-(Hg), berzelianite and uraninite. Arsenoústalečite is dark grey, with a metallic lustre. Mohs hardness is *ca.* 3½–4; calculated density is 5.730 g/cm³. In reflected light, arsenoústalečite is pale grey with a yellowish shade; it is isotropic. Internal reflections were not observed. Reflectance values for the four COM wavelengths in air [R (%) λ (nm)] are: 33.3 (470); 33.1 (546); 33.0 (589); and 32.9 (650). The empirical formula of arsenoústalečite is $(Cu_{5.81}Ag_{0.17})_{\Sigma5.98}(Cu_{5.95}Fe_{0.02}Zn_{0.02}Hg_{0.01})_{\Sigma6.00}(As_{1.40}Sb_{0.87}Te_{1.73})_{\Sigma4.00}(Se_{10.30}S_{2.32})_{\Sigma12.61}$. The ideal formula is $Cu_{12}(As_2Te_2)Se_{13}$, which requires (in wt.%) Cu 34.76, As 6.83, Te 11.63, Se 46.78, total 100.00. Arsenoústalečite is cubic, $I\bar{4}3m$, with unit-cell parameters $a = 10.6580(19)$ Å, $V = 1210.7(6)$ Å³ and $Z = 2$. The strongest reflections of the calculated powder X-ray diffraction pattern [d, Å (I, %) *hkl*] are: 3.077 (100) 222, 2.848 (10) 321, 1.946 (12) 521, 1.884(52) 440 and 1.608(21) 622. According to the single-crystal X-ray diffraction data ($R_1 = 0.0285$ on the basis of 334 unique reflections with $F_o > 4\sigma F_o$ and 24 refined parameters), arsenoústalečite is isotypic with other tetrahedrite-group minerals. The crystal structure of co-existing stibioústalečite, with an empirical formula of $(Cu_{5.69}Ag_{0.07})_{\Sigma5.76}(Cu_{5.80}Zn_{0.13}Fe_{0.06}Hg_{0.01})_{\Sigma6.00}(Sb_{1.82}As_{0.42}Te_{1.76})_{\Sigma4.00}(Se_{9.52}S_{3.10})_{\Sigma12.62}$ and unit-cell parameters $a = 10.6975(16)$ Å, $V = 1224.2(5)$ Å³ and $Z = 2$, was refined to $R_1 = 0.0191$ on the basis of 267 unique reflections with $F_o > 4\sigma F_o$ and 24 refined parameters. Structural relationships and crystal-chemistry of both members of the ústalečite series are discussed. Arsenoústalečite is named after its type locality, the Ústaleč deposit and its chemical composition. The mineral and its name have been approved by the Commission on New Minerals, Nomenclature and Classification of the International Mineralogical Association (IMA2022-116).

Keywords: arsenoústalečite; new mineral; selenide; copper; arsenic; tellurium; crystal structure; stibioústalečite; Ústaleč; Czech Republic

Introduction

The tetrahedrite group shows the widest chemical variability among sulfosalts, as proven by the currently 38 valid mineral species reported in the official List of Mineral Names of the Commission on New Minerals, Nomenclature and Classification of the International Mineralogical Association (IMA-CNMNC, Pasero, 2023, updated July 2023). This is a consequence of the plasticity of the crystal structure of tetrahedrite isotypes, able to accommodate several homo- and heterovalent substitutions, hosting many chemical constituents typical of hydrothermal ore deposits (Moëlo *et al.*, 2008; Biagioni *et al.*, 2020). The general structural formula of tetrahedrite-group minerals can be written as $^{M(2)}A_6{}^{M(1)}(B_4C_2)_{\Sigma6}{}^{X(3)}D_4{}^{S(1)}Y_{12}{}^{S(2)}Z$, where $A = Cu^+$, Ag^+ and $\square$ (vacancy); $B = Cu^+$, and Ag^+; $C = Zn^{2+}$, Fe^{2+}, Hg^{2+}, Cd^{2+}, Ni^{2+},

Mn^{2+}, Cu^{2+}, Cu^+, In^{3+} and Fe^{3+}; $D = Sb^{3+}$, As^{3+}, Bi^{3+}, and Te^{4+}; $Y = S^{2-}$, and Se^{2-}; and $Z = S^{2-}$, Se^{2-} and $\square$ (Biagioni *et al.*, 2020).

Within this group, members of the tetrahedrite and tennantite series are the most common, whereas species having Se as the dominant anion or Te as the D chemical constituent are rare or very rare. Indeed, Se and Te are two among the chemical constituents of tetrahedrite-group minerals showing the lowest concentration in the Earth's continental crust, i.e. 120 and 5 ng/g, respectively (Wedepohl, 1995). Cadmium (100 ng/g), Ag (70 ng/g), In (50 ng/g) and Hg (40 ng/g) are rarer than Se (Wedepohl, 1995), but some of them (Ag and Hg) are particularly widespread in hydrothermal environments and are able to become dominant constituents. As discussed by Christy (2015), Ag and Hg, as well as Se, can be considered as anomalously abundant elements, whereas Cd and In are dispersed elements, owing to their geochemical behaviour. Tellurium is exceptional, being concentrated in more than 150 different mineral species notwithstanding its extreme low abundance in Nature (Christy, 2015).

Tellurium-rich members of the tetrahedrite group have been known for a long time. The first descriptions of goldfieldite were

given by Sharwood (1907) and Ransome (1909). Thompson (1946) proved this mineral to be isotypic with tetrahedrite. Kato and Sakurai (1970) and Kalbskopf (1974) found that Te does not substitute for S but replaces Sb and As. Several authors have debated the actual definition of goldfieldite (e.g. Trudu and Knittel, 1998) and the debate was finally solved in the nomenclature of the tetrahedrite group by Biagioni *et al.* (2020). Increased Se-contents in Te-rich members was, until recently, only known in samples from the epithermal Au deposits in Kamchatka, Russia (Spiridonov and Okrugin, 1985; Pohl *et al.*, 1996; Spiridonov *et al.*, 2014), and from the Wild Dog epithermal Au system on Bougainville Island, Papua New Guinea (Noviello, 1989). In these findings, Se does not exceed 3.0 atoms per formula unit (apfu). The experiments carried out at 340°C by de Medicis and Giasson (1971) on the system Cu−Te−Se failed to produce the Se-bearing analogues of goldfieldite. The first Se- and Te-dominant member of the tetrahedrite group, stibioústalečite, was described from a selenide association from the Ústaleč mine near Horažďovice (Czech Republic) by Sejkora *et al.* (2022). In this association, a mineral with As > Sb, i.e. the As-analogue of stibioústalečite, was also detected (Sejkora *et al.*, 2022). Further chemical and crystallographic investigations confirmed such a preliminary identification, allowing the proposal of the new mineral species arsenoústalečite.

This new mineral and its name (symbol Aúč) were approved by the Commission on New Minerals, Nomenclature and Classification of the International Mineralogical Association (IMA2022-116). Arsenoústalečite ('*arseno-oostaletchite*') is named after its type locality, the Ústaleč deposit near Horažďovice, Czech Republic, and its chemical composition, being the (As/Te) end-member in the ústalečite series. The holotype material (polished section) is deposited in the mineralogical collection of the Department of Mineralogy and Petrology of the National Museum, Prague, Czech Republic (catalogue number P1P 7/2021). It is worth noting that it is the same type material containing stibioústalečite (Sejkora *et al.*, 2022). The crystal used for the single-crystal X-ray diffraction study is kept in the mineralogical collection of the Museo di Storia Naturale of the Università di Pisa, Via Roma 79, Calci (PI), Italy, under catalogue number 20026.

As the studied material also contained stibioústalečite, a grain of this recently approved species suitable for single-crystal X-ray diffraction study was sought and found in this investigation. In addition, Sejkora *et al.* (2022) had not been successful in refining the crystal structure of this species, owing to the extremely low diffraction intensities, resulting in a value of R_{int} = 0.214.

In this paper the description of arsenoústalečite and details of the crystal structure of its Sb-isotype stibioústalečite are reported, along with discussion on some crystal-chemical and nomenclature issues.

Occurrence and mineral description

Occurrence

Arsenoústalečite was found at the small Ústaleč uranium deposit, mined by the (now abandoned) Ústaleč mine, located 500 m northeast of the village Ústaleč, 15 km west of Horažďovice, SW Bohemia, Czech Republic (GPS coordinates: 49°19′15.04″N, 13°30′21.40″E).

The Ústaleč uranium deposit belongs to the Horažďovice uranium district and it is similar to several analogous ore deposits and occurrences including Újezd u Kasejovic, Nalžovské Hory, Těchonice and others. The hydrothermal uranium mineralisation

is structurally controlled by the regional Horažďovice fault zone trending WNW−ESE. The deposit is hosted in metamorphic rocks of the Varied Group of the Moldanubian Complex at the contact with the Chanovice apophysis of the Central Bohemian Plutonic Complex (Litochleb *et al.*, 1999). More details of the geological setting of the Ústaleč uranium deposit are given in Sejkora *et al.* (2022).

Arsenoústalečite was identified in the selenide mineralisation whose occurrence is intimately related to white or yellowish, post-ore calcite (younger than uranium mineralisation). Selenides penetrate uraninite along grain interfaces and at places they overgrow or replace spheroidal uraninite aggregates. Litochleb *et al.* (1999) described from here berzelianite, bukovite, clausthalite, eskebornite, eucairite, ferroselite, 'hakite', 'giraudite', chaméanite and umangite. Recently, the study of ore samples from this locality allowed the definition of the new mineral species stibioústalečite (Sejkora *et al.*, 2022) as well as the refinement of the crystal structure of bukovite (Sejkora *et al.*, 2023b). Moreover, other interesting selenides have been identified, i.e. athabascaite, bytízite, crookesite, hakite-(Hg), klockmannite and the not-yet approved 'hakite-(Cu)'.

Arsenoústalečite was identified in the type material of stibioústalečite, represented by a sample of calcite gangue where it is associated with hakite-(Hg), stibioústalečite, berzelianite and uraninite. The crystallisation of arsenoústalečite is probably related to the circulation of low-temperature hydrothermal fluids during the late-stage evolution of the Ústaleč uranium deposit.

Physical and optical properties

Arsenoústalečite occurs as anhedral grains up to 40 μm in size and forms part (up to 100 μm in size) of arsenoústalečite/stibioústalečite aggregates (Fig. 1). The mineral is dark grey in colour and opaque in transmitted light; it has a metallic lustre. The Mohs hardness is close to 3½−4, in agreement with other members of the tetrahedrite group. Arsenoústalečite is brittle, with an indistinct cleavage and a conchoidal fracture. Density was not measured, owing to the small amount of available material;
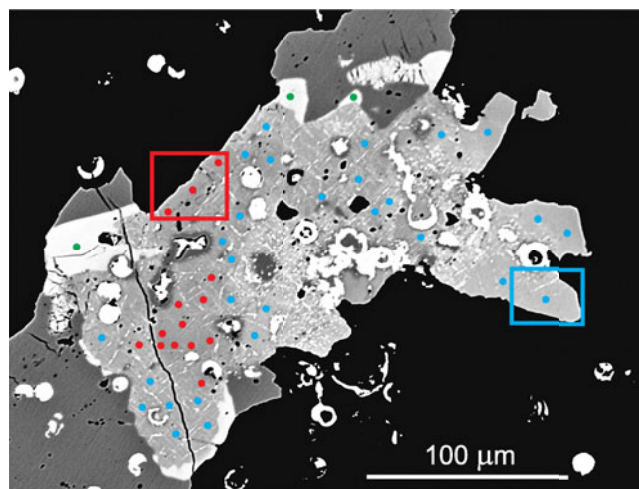
Figure 1. Back-scattered electron (BSE) image of the sample studied containing arsenoústalečite (red circles), stibioústalečite (blue circles), hakite-(Hg) (green circles), berzelianite (dark grey in BSE) and uraninite (white in BSE). The grains used for single-crystal X-ray diffraction study were extracted from the red (arsenoústalečite) and blue (stibioústalečite) boxes. Holotype sample.

on the basis of the empirical formula ($Z = 2$) and the single-crystal unit-cell parameters, the calculated density is 5.730 g/cm^3. In reflected light, arsenoústalečite is isotropic, pale grey with a yellowish shade. Internal reflections were not observed. Reflectance spectra were measured in air with a TIDAS MSP400 spectrophotometer attached to a Leica microscope (50× objective) using a WTiC (Zeiss no. 370) standard, with a square sample measurement field of *ca.* 10×10 μm. The results for the 400–700 nm range are given in Table 1 and plotted in Fig. 2 in comparison with data for members of the ústalečite and goldfieldite series.

Chemical composition

Chemical analyses were performed using a Cameca SX100 electron microprobe (National Museum, Prague) operating in wavelength-dispersive mode (25 kV, 20 nA and 1 μm wide beam). The following standards and X-ray lines were used to minimise line overlap: Ag (Ag*L*α), Au (Au*M*α), Bi (Bi*M*β), CdTe (Cd*L*α), Co (Co*K*α), chalcopyrite (Cu*K*α), pyrite (Fe*K*α, S*K*α), HgTe (Hg*M*α), NiAs (Ni*K*α, As*L*β), PbS (Pb*M*α), PbSe (Se*L*α), PbTe (Te*L*α), Sb$_2$S$_3$ (Sb*L*α), Tl(Br,I) (Tl*L*α) and ZnS (Zn*K*α). Peak counting times were 20 s for all elements and one half of the peak time for each background. Some elements, such as Au, Bi, Co, Ni and Pb were found to be below the detection limits (0.02–0.10 wt.%). Raw intensities were converted to the concentrations of elements using the automatic 'PAP' (Pouchou and Pichoir, 1985) matrix-correction software.

Analytical data for arsenoústalečite (average of 11 analyses) are given in Table 2. On the basis of (As + Sb + Te) = 4 atoms per formula unit (apfu), the empirical chemical formula is $^{M(2)}$(Cu$_{5.81}$Ag$_{0.17}$)$_{\Sigma5.98}$ $^{M(1)}$(Cu$_{5.95}$Fe$_{0.02}$Zn$_{0.02}$Hg$_{0.01}$)$_{\Sigma6.00}$ $^{X(3)}$(As$_{1.40}$Sb$_{0.87}$Te$_{1.73}$)$_{\Sigma4.00}$ $^{S(1)+S(2)}$(Se$_{10.30}$S$_{2.32}$)$_{\Sigma12.61}$. The ideal formula is Cu$_{12}$(As$_2$Te$_2$)Se$_{13}$, which requires (in wt.%) Cu 34.76, As 6.83, Te 11.63, Se 46.78, total 100.00. The chemical composition (average of 4 spot analyses) of the co-existing stibioústalečite grain used for single-crystal measurement (Table 2) corresponds to the empirical formula $^{M(2)}$(Cu$_{5.69}$Ag$_{0.07}$)$_{\Sigma5.76}$ $^{M(1)}$(Cu$_{5.80}$Zn$_{0.13}$Fe$_{0.06}$Hg$_{0.01}$)$_{\Sigma6.00}$ $^{X(3)}$(Sb$_{1.82}$As$_{0.42}$Te$_{1.76}$)$_{\Sigma4.00}$ $^{S(1)+S(2)}$(Se$_{9.52}$S$_{3.10}$)$_{\Sigma12.62}$.
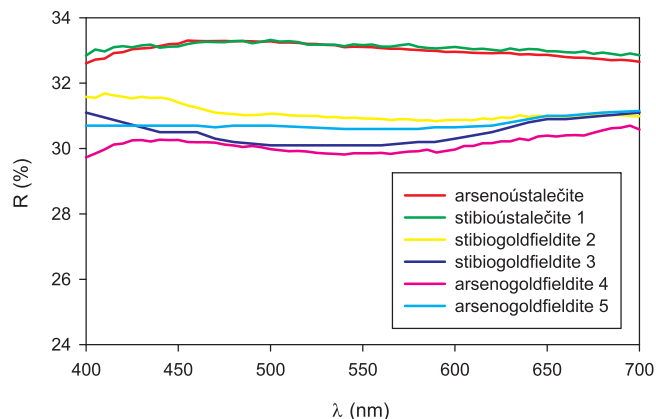
X-ray diffraction data

Grains of arsenoústalečite and stibioústalečite were extracted from the polished section studied previously using electron microprobe analysis (Fig. 1) and mounted on a carbon fibre for examination

Figure 2. Reflectance curve for arsenoústalečite from Ústaleč. For the sake of comparison, the curves for stibioústalečite (1) from Ústaleč (Sejkora et al., 2022), stibiogoldfieldite (2) from the Mohawk mine (Biagioni et al., 2022), stibiogoldfieldite (3) from Goldfield (Criddle and Stanley 1993, p. 208, described as 'goldfieldite'), arsenogoldfieldite (4) from the North Star mine (IMA 2022-084; Sejkora et al., 2023a) and arsenogoldfieldite (5) from the Tramway mine (Criddle and Stanley 1993, p. 209, described as 'goldfieldite') are shown.

with a Bruker D8 Venture single-crystal X-ray diffractometer equipped with an air-cooled Photon III area detector and micro-focus Mo*K*α radiation (Centro per l'Integrazione della Strumentazione Scientifica dell'Università di Pisa, University of Pisa). The detector-to-crystal distance was set to 38 mm for both samples and data were collected using φ scan modes in 0.5° slices. Data were integrated with the Bruker *SAINT* software package using a narrow-frame algorithm and corrected for Lorentz-polarisation, absorption and background. The crystal structure of both arsenoústalečite and stibioústalečite were refined using *Shelxl*-2018 (Sheldrick, 2015), starting from the atomic coordinates of stibiogoldfieldite given by Biagioni *et al.* (2022). The following neutral scattering curves, taken from the *International Tables for Crystallography* (Wilson, 1992) were used: Cu *vs.* ☐ (vacancy) at M(2), Cu *vs.* ☐ at M(1), As *vs.* Te at X(3), Se *vs.* S at the S(1) and S(2) sites. The occurrence of racemic twinning was modelled. Crystal structure refinements are described below, whereas further details on data collection and refinement are given in Table 3. Fractional atom coordinates and equivalent isotropic parameters are reported in Table 4, whereas Table 5 shows selected bond distances. Weighted bond-valence sums, calculated using the bond-parameters of

Table 1. Reflectance values (%) for arsenoústalečite.*

λ (nm)	*R* (%)	λ (nm)	*R* (%)
400	32.6	560	33.1
420	32.9	580	33.0
440	33.1	**589**	**33.0**
460	33.3	600	33.0
470	**33.3**	620	32.9
480	33.3	640	32.9
500	33.3	**650**	**32.9**
520	33.2	660	32.8
540	33.1	680	32.7
546	**33.1**	700	32.7

*The reference wavelengths required by the Commission on Ore Mineralogy (COM) are given in bold.

Table 2. Chemical data (wt.%) for arsenoústalečite and co-existing stibioústalečite.

Constituent	Arsenoústalečite ($n = 11$)			Stibioústalečite ($n = 4$)		
	mean	range	(σ)	mean	range	(σ)
Cu	35.55	35.03–35.89	0.27	34.60	34.05–34.87	0.38
Ag	0.87	0.25–1.65	0.50	0.35	0.09–1.00	0.43
Fe	0.06	0.00–0.10	0.03	0.15	0.00–0.24	0.11
Zn	0.06	0.00–0.12	0.04	0.41	0.07–0.77	0.29
Hg	0.09	0.00–0.60	0.19	0.12	0.06–0.21	0.07
As	5.00	4.47–5.26	0.22	1.48	0.69–2.31	0.74
Sb	5.04	4.43–7.13	0.75	10.50	9.45–11.24	0.76
Te	10.50	8.97–10.95	0.53	10.65	9.54–12.37	1.23
S	3.54	3.22–3.81	0.17	4.71	3.30–5.78	1.04
Se	38.70	38.27–39.24	0.28	35.62	34.26–37.29	1.25
Total	99.41			98.59		

(σ) – estimated standard deviation; *n* = number of spot analyses.

Table 3. Summary of data collection conditions and refinement parameters for arsenoústalečite and stibioústalečite.

	Arsenoústalečite	Stibioústalečite
Crystal data		
Crystal size (mm)	0.025 × 0.020 × 0.020	0.035 × 0.020 × 0.015
Cell setting, space group	Cubic, $I\bar{4}3m$	
a (Å)	10.6580(19)	10.6975(16)
V (Å^3)	1210.7(6)	1224.2(5)
Z	2	2
Data collection and refinement		
Radiation, wavelength (Å)	Mo$K\alpha$, $\lambda = 0.71073$	
Temperature (K)	293(2)	
$2\theta_{max}$ (°)	66.44	54.814
Measured reflections	2640	2114
Unique reflections	410	283
Reflections with $F_o > 4\sigma(F_o)$	334	267
R_{int}	0.0473	0.0393
$R\sigma$	0.0331	0.0235
Range of h, k, l	$-13 \le h \le 13$,	$-13 \le h \le 13$,
	$-14 \le k \le 9$,	$-12 \le k \le 12$,
	$-13 \le l \le 13$	$-8 \le l \le 13$
R [$F_o > 4\sigma(F_o)$]	0.0285	0.0191
R (all data)	0.0452	0.0219
wR (on F_o^2)[1]	0.0512	0.0346
Goof	1.070	1.174
Flack parameter[2]	−0.03(6)	0.05(4)
Number of least-squares parameters	24	24
Maximum and	1.39 [at 2.26 Å from S(1)]	0.45 [at 1.46 Å from S(1)]
minimum residual peak (e Å^{-3})	−0.92 [at 1.71 Å from S(1)]	−0.46 [at 1.92 Å from M(1)]

[1] $w = 1/[\sigma^2(F_o^2) + (0.0130P)^2 + 4.6919P]$ for arsenoústalečite; $w = 1/[\sigma^2(F_o^2) + 3.6510P]$ for stibioústalečite.
[2] Flack (1983)

Brese and O'Keeffe (1991), are given in Table 6. For both arsenoústalečite and stibioústalečite, Crystallographic Information Files (CIF) have been deposited with the Principal Editor of *Mineralogical Magazine* and are available as Supplementary Materials.

Arsenoústalečite
Intensity data were collected using a short prismatic fragment, $25 \times 20 \times 20$ μm in size. A total of 188 frames was collected with an exposure time of 40 s per frame. Unit-cell parameters,

Table 4. Site, site occupancy, fractional atom coordinates, equivalent isotropic displacement parameters (Å^2) for arsenoústalečite and stibioústalečite.

Arsenoústalečite

Site	Site occupancy	x/a	y/b	z/c	U_{eq}
$M(2a)$	Cu$_{0.758(9)}$	0.2090(3)	0	0	0.0480(15)
$M(2b)$	Cu$_{0.121(5)}$	0.2111(12)	−0.0662(18)	0.0662(18)	0.0480(15)
$M(1)$	Cu$_{1.00}$	¼	½	0	0.0311(8)
$X(3)$	Te$_{0.614(17)}$As$_{0.386(17)}$	0.26226(8)	0.26226(8)	0.26226(8)	0.0210(5)
$S(1)$	Se$_{0.859(13)}$S$_{0.141(13)}$	0.11269(10)	0.11269(10)	0.36001(12)	0.0207(4)
$S(2)$	S$_{0.69(3)}$Se$_{0.31(3)}$	0	0	0	0.031(2)

Stibioústalečite

Site	Site occupancy	x/a	y/b	z/c	U_{eq}
$M(2a)$	Cu$_{0.83(4)}$	0.7920(3)	0	0	0.051(4)
$M(2b)$	Cu$_{0.08(2)}$	0.790(2)	0.050(5)	−0.050(5)	0.051(4)
$M(1)$	Cu$_{1.00}$	¾	½	0	0.0280(8)
$X(3)$	Te$_{0.963(18)}$As$_{0.037(18)}$	0.73637(7)	0.73637(7)	0.73637(7)	0.0178(4)
$S(1)$	Se$_{0.935(14)}$S$_{0.065(14)}$	0.88846(10)	0.88846(10)	0.63883(12)	0.0194(5)
$S(2)$	S$_{0.76(3)}$Se$_{0.24(3)}$	0	0	0	0.032(3)

Table 5. Selected bond distances (in Å) for arsenoústalečite and stibioústalečite.

	Arsenoústalečite	Stibioústalečite
$M(1)$–S(1) ×4	2.4104(9)	2.4132(9)
$M(2a)$–S(2)	2.227(3)	2.225(3)
$M(2a)$–S(1) ×2	2.340(2)	2.352(3)
$M(2b)$–S(2)	2.461(14)	2.37(3)
$M(2b)$–S(1) ×2	2.530(15)	2.45(3)
$X(3)$–S(1) ×3	2.4835(14)	2.5265(14)

refined on the basis of the XYZ centroids of 699 reflections above 20 σI with $9.369 < 2\theta < 59.87°$, are $a = 10.6580(19)$ and $V = 1210.7(6)$ Å^3.

Several cycles of isotropic refinement, with full occupancies of Cu at $M(2)$ and $M(1)$, of Te at $X(3)$, and Se at S(1) and S(2), converged to $R_1 = 0.0873$, thus indicating the correctness of the structural model. However, the Flack parameter (Flack, 1983) was 0.83(16), thus indicating the necessity to invert the structure. At this stage of the refinement, a high maximum residual close to the $M(2)$ position was found. After its addition as the split site $M(2b)$, the R_1 value decreased to 0.0625, constraining the displacement parameter of the two sub-sites to be the same. The S(2) site showed a high U_{iso}, thus indicating a significant replacement of Se by S. At this stage of refinement, the neutral scattering curves reported above were used, refining mixed occupancies at $X(3)$, S(1) and S(2) sites. As chemical data indicated the occurrence of minor Ag, the site occupancies at $M(2a)$ and $M(2b)$ were freely refined but their sum did not deviate from the full occupancy by Cu. Similarly, the free refinement of the site occupancy at the $M(1)$ site indicated the full occupancy by Cu. For this reason, the sum of site occupancies of $M(2a)$ and $M(2b)$ was constrained to be one, whereas the site occupancy at $M(1)$ was fixed to one. The refinement of this isotropic structural model converged to $R_1 = 0.0450$. The anisotropic modelling of the displacement parameters of cation sites lowered the R_1 to 0.0308. At the final stage of refinement, a full anisotropic model was assumed. It converged to $R_1 = 0.0285$ for 334 reflections with $F_o > 4\sigma(F_o)$ and 24 refined parameters.

Powder X-ray diffraction data of arsenoústalečite could not be collected, due to the paucity of available material. Consequently, powder X-ray diffraction data, given in Table 7, were calculated

Table 6. Weighted bond-valence sums (in valence units) in arsenoústalečite and stibioústalečite.

Arsenoústalečite

Site	$M(1)$	$M(2a)$	$M(2b)$	$X(3)$	Σani.	theor.
S(1)	$^{2×→}0.33^{×4↓}$	$0.30^{×2↓}$	$0.03^{×2↓}$	$1.00^{×3↓}$	1.99	2.00
S(2)		$^{6×→}0.33$	$^{12×→}0.03$		2.34	2.00
Σcat.	1.32	0.93	0.09	3.00		
theor.	1.00	0.76	0.12	3.45		

Stibioústalečite

Site	$M(1)$	$M(2a)$	$M(2b)$	$X(3)$	Σani.	theor.
S(1)	$^{2×→}0.34^{×4↓}$	$0.35^{×2↓}$	$0.02^{×2↓}$	$1.01^{×3↓}$	2.06	2.00
S(2)		$^{6×→}0.33$	$^{12×→}0.02$		2.22	2.00
Σcat.	1.36	1.03	0.06	3.03		
theor.	1.00	0.83	0.08	3.40		

Note: left and right superscripts indicate the number of equivalent bonds involving cations and anions, respectively. cat = cations; ani = anions.

Table 7. Calculated powder X-ray diffraction data for arsenoústalečite.

I_{calc}	d_{calc}	h k l	I_{calc}	d_{calc}	h k l
1	5.329	2 0 0	**12**	**1.946**	**5 2 1**
4	4.351	2 1 1	**52**	**1.884**	**4 4 0**
6	3.768	2 2 0	5	1.828	4 3 3
3	3.370	3 1 0	1	1.828	5 3 0
100	**3.077**	**2 2 2**	1	1.776	4 4 2
10	**2.848**	**3 2 1**	1	1.729	5 3 2
2	2.664	4 0 0	7	1.729	6 1 1
4	2.512	3 3 0	2	1.685	6 2 0
7	2.512	4 1 1	**21**	**1.608**	**6 2 2**
2	2.383	4 2 0	1	1.507	5 5 0
1	2.272	3 3 2	1	1.507	5 4 3
3	2.176	4 2 2	2	1.507	7 1 0
1	2.090	5 1 0	1	1.450	6 3 3
6	2.090	4 3 1			

Intensity and d_{hkl} (in Å) were calculated using the software *PowderCell*2.3 (Kraus and Nolze, 1996) on the basis of the structural data given in Tables 3 and 4. Only reflections with $I_{rel.} \geq 1$ are listed. The five strongest reflections are given in bold.

using the software *PowderCell* 2.3 (Kraus and Nolze, 1996) on the basis of the structural model given in Tables 3 and 4.

Stibioústalečite

Intensity data were collected using a short prismatic fragment, $35 \times 20 \times 15$ μm in size. A total of 188 frames was collected with an exposure time of 30 s per frame. Unit-cell parameters, refined on the basis of the XYZ centroids of 842 reflections above 20 σI with $7.619 < 2\theta < 54.813°$, are $a = 10.6975(16)$ and $V = 1224.2(5)$ Å³.

Several cycles of isotropic refinement, with full occupancies of Cu at $M(2)$ and $M(1)$, of Te at $X(3)$, and Se at $S(1)$ and $S(2)$, converged to $R_1 = 0.0686$, thus indicating the correctness of the structural model. Also the Flack parameter (Flack, 1983), i.e. 0.04(15), indicated the goodness of the model. At this stage of the refinement, a relatively high maximum residual close to the $M(2)$ position was found. After its addition as the split site $M(2b)$, the R_1 value decreased to 0.0430, constraining the displacement parameters of the two sub-sites to be the same. The U_{iso} at the $S(2)$ site was too high, suggesting a significant replacement of Se by S. At this stage of refinement, mixed occupancies at $X(3)$, $S(1)$ and $S(2)$ sites were refined. As chemical data indicated the occurrence of minor Ag at $M(2)$, the site occupancies at $M(2a)$ and $M(2b)$ were freely refined but their sum did not deviate from the full occupancy by Cu. Analogously, the $M(1)$ site was fully occupied by Cu. The refinement of this isotropic structural model converged to $R_1 = 0.0287$. The anisotropic modelling of the displacement parameters of cation sites lowered the R_1 to 0.0210. At the final stage of refinement, a full anisotropic model was assumed. It converged to $R_1 = 0.0191$ for 267 reflections with $F_o > 4\sigma(F_o)$ and 24 refined parameters.

Results and discussion

Crystal structures of arsenoústalečite and stibioústalečite

The crystal structures of arsenoústalečite and stibioústalečite agree with the general features of the members of the tetrahedrite isotypic group (Biagioni *et al.*, 2020), i.e. a three-dimensional framework formed by corner-sharing $M(1)$-centred tetrahedra with cages hosting $S(2)$-centred $M(2)_6$-octahedra, encircled by four $X(3)S(1)_3$ trigonal pyramids. As observed in other tetrahedrite-group isotypes (e.g. Andreasen *et al.*, 2008; Welch *et al.*, 2018),

the $M(2)$ site is split into two sub-positions, namely $M(2a)$ and $M(2b)$.

Cation sites

The tetrahedrally coordinated $M(1)$ site has an average bond distance of 2.410 Å in arsenoústalečite and 2.413 Å in stibioústalečite. These values are longer than the $M(1)$–$S(1)$ distance observed in stibiogoldfieldite, i.e. 2.329 Å (Biagioni *et al.*, 2022). The distances observed in the members of the ústalečite series are similar to the Cu–Se distance reported for other Cu-centred tetrahedra coordinated by Se, e.g. 2.421 Å in eskebornite (Delgado *et al.*, 1992). Electron microprobe data allows us to hypothesise the following site occupancies at the $M(1)$ site of arsenoústalečite and stibioústalečite (with rounding errors): $(Cu_{0.992}Fe_{0.003}Zn_{0.003}Hg_{0.002})$ and $(Cu_{0.967}Zn_{0.022}Fe_{0.010}Hg_{0.001})$, respectively, corresponding to mean atomic numbers (MAN) of 29.10 and 29.04 electrons. In both cases, the site occupancy at $M(1)$ site was refined as a pure Cu site, i.e. a MAN value of 29 electrons. Bond-valence sums at the $M(1)$ site of arsenoústalečite and stibioústalečite are 1.32 and 1.36 valence units (vu) (Table 6). Such overbonding at the tetrahedrally coordinated site in tetrahedrite-group minerals is a well known feature (e.g. Welch *et al.*, 2018).

As described above, in both arsenoústalečite and stibioústalečite, the $M(2)$ site is split into two sub-positions, $M(2a)$ and $M(2b)$, separated by 1.00(3) Å in the former and 0.75(8) Å in the latter, with the distance of two neighbouring $M(2b)$ positions of 1.99(6) Å and 1.51(16) Å, respectively. The $M(2b)$ positions are at 2.60(3) and 2.84(8) Å from the $X(3)$ site. These distances are definitely longer than that reported by Makovicky *et al.* (2005) in Cu-rich unsubstituted tennantite, where a $M(2b)$–$X(3)$ distance of 2.41 Å was observed, suggesting a possible interaction between the lone-pair electrons of As and Sb and the valence shells of Cu. The atom hosted at the $M(2a)$ position shows a triangular planar coordination, whereas at $M(2b)$ the coordination is a flat trigonal pyramid. In arsenoústalečite, average bond distances are 2.302 Å and 2.507 Å for $M(2a)$ and $M(2b)$, respectively; in its Sb-isotype such values are 2.310 Å and 2.42 Å, respectively. These values are larger than those observed in stibiogoldfieldite, having an average bond distance of 2.251 Å (Biagioni *et al.*, 2022), owing to the replacement of S by Se. The $M(2a)$ and $M(2b)$ sub-sites were modelled as occupied by Cu only; indeed, minor Ag ($\sim$0.03 and 0.01 atoms per site in arsenoústalečite and stibioústalečite, respectively) occurs. No detectable vacancy at these sites were observed. The sum of the bond-valence for $M(2a) + M(2b)$ (Table 6) is 1.02 and 1.09 vu for arsenoústalečite and stibioústalečite, respectively, in agreement with the presence of monovalent Cu.

The $X(3)$ site has an average bond distance of 2.484 Å and 2.526 Å in arsenoústalečite and stibioústalečite, respectively. In stibiogoldfieldite, the distance is 2.390 Å with the site occupancy $(Sb_{0.28}As_{0.16}Bi_{0.06}Te_{0.50})$ (Biagioni *et al.*, 2022). The refined MAN at the $X(3)$ site of the As- and Sb-isotypes of the ústalečite series are 44.67 and 51.30 electrons, to be compared with those calculated from electron microprobe analyses, i.e. 45.13 and 49.64 electrons for arsenoústalečite and stibioústalečite, respectively, on the basis of the proposed site occupancies $(As_{0.35}Sb_{0.22}Te_{0.43})$ and $(Sb_{0.46}As_{0.10}Te_{0.44})$. Using the ideal bond valences and bond valence parameters of Brese and O'Keeffe (1991), the average distance of 2.43 Å and 2.48 Å can be calculated for arsenoústalečite and stibioústalečite, shorter than the observed ones. The weighted bond-valence sum at $X(3)$, i.e. 3.00 and 3.03 vu for arsenoústalečite

and stibioústalečite, are lower than the expected values based on the proposed site occupancies (Table 6).

Anion sites

The S(1) site is tetrahedrally coordinated by two $M(1)$ site, one $M(2)$ site [i.e. $M(2a)$ or one of the two mutually exclusive $M(2b)$ positions], and one $X(3)$ site. The refined site occupancy at S(1) is $Se_{0.859}S_{0.141}$ in arsenoústalečite and $Se_{0.935}S_{0.065}$ in stibioústalečite, with bond-valence sums of 1.99 and 2.06 vu, respectively (Table 6).

The S(2) site is octahedrally coordinated by six atoms hosted at $M(2a)+M(2b)$. In both arsenoústalečite and stibioústalečite this site is S-dominant, with site occupancies $S_{0.69}Se_{0.31}$ and $S_{0.74}Se_{0.26}$, respectively. This site is slightly overbonded, with bond-valence sums of 2.34 and 2.22 vu (Table 6), probably as a consequence of too short $M(2)$–Se distances.

It is interesting to compare the S/(S + Se) atomic ratios obtained through the crystal structure refinement with those measured through the electron microprobe analysis. In arsenoústalečite, electron microprobe data gave $(Se_{10.30}S_{2.32})_{\Sigma 12.61}$, with a ratio of 0.184. Taking into account the site multiplicity, the anion content $(Se_{10.62}S_{2.38})$ can be obtained from structural analysis, having a S/(S + Se) ratio of 0.183, in agreement with chemical data. In stibioústalečite, a higher S content was detected through electron microprobe analysis, with a S/(S + Se) ratio of 0.246. Crystal structure refinement points to an undeniably lower ratio, 0.118; in type stibioústalečite such a ratio was 0.198 (Sejkora *et al.*, 2022).

Crystal chemistry of arsenoústalečite and stibioústalečite

Arsenoústalečite and its Sb-isotype stibioústalečite (Sejkora *et al.*, 2022) are new additions to the selenide minerals belonging to the tetrahedrite group, along with members of the hakite series, giraudite-(Zn) and pošepnýite. Moreover, they are the first Te–Se species of this group and are isotypic with arsenogoldfieldite and stibiogoldfieldite (Table 8).

Pohl *et al.* (1996) first refined the crystal structure of a Se-bearing stibiogoldfieldite using the Rietveld method. They observed an increase in the unit-cell parameters owing to the Se–S substitution. Indeed, they reported *a* values ranging between 10.32 and 10.34 Å, larger than those of arsenogoldfieldite (*a* = 10.29 Å − Sejkora *et al.*, 2023a) and similar to those of stibiogoldfieldite from the Mohawk mine (*a* = 10.35 Å − Biagioni *et al.*, 2022). In fact, the unit-cell parameters of Te-rich members of the tetrahedrite group are a function of their complex crystal chemistry (e.g. Makovicky and Karup-Møller, 2017). It is interesting to observe that the difference in unit-cell parameters between As- and Sb-members of the goldfieldite series is limited (~0.07 Å for Te = 2 apfu in synthetic products − Makovicky and

Karup-Møller, 2017). The difference in the *a* unit-cell parameter of arsenoústalečite and stibioústalečite is ~0.04 Å. This value seems to be in keeping with the observations on synthetic members of the goldfieldite series and does not agree with the large *a* value reported by Sejkora *et al.* (2022), i.e. 10.83 Å, with a variation of 0.17 Å with respect to arsenoústalečite. For this reason, the calculated density of stibioústalečite, given by Sejkora *et al.* (2022) as 5.676 g/cm³, should be revised to ~5.89 g/cm³.

The Rietveld refinements of Pohl *et al.* (1996) gave another interesting result. According to them, Se is hosted at the S(1) site, whereas it was not possible to accurately determine the actual occupancy of S(2). The results obtained on both members of the ústalečite series agrees with the work of Pohl *et al.* (1996), clearly indicating that Se is preferentially partitioned at S(1), with S(2) being a dominant S-position. For this reason, the end-member formulae of the studied material are $^{M(2)}Cu_6{}^{M(1)}Cu_6{}^{X(3)}(As_2Te_2)_{\Sigma 4}{}^{S(1)}Se_{12}{}^{S(2)}S (Z=2)$ and $^{M(2)}Cu_6{}^{M(1)}Cu_6{}^{X(3)}(Sb_2Te_2)_{\Sigma 4}{}^{S(1)}Se_{12}{}^{S(2)}S$ $(Z=2)$ for arsenoústalečite and stibioústalečite, respectively.

This result has a two-fold implication, being interesting from the point of view of mineral systematics (i.e. nomenclature issues) as well as for the genesis of members of the ústalečite series.

Nomenclature issues

Sejkora *et al.* (2022) first introduced the ústalečite series, following the classification scheme proposed by Biagioni *et al.* (2020) for Te-bearing minerals of the tetrahedrite group and extending it to the Se-isotypes. The nomenclature scheme of Sejkora *et al.* (2022) is:

(1) hakite/giraudite, with 0 < Te (apfu) < 1;
(2) new names − stibioústalečite (Sejkora *et al.*, 2022) and arsenoústalečite (this paper) for composition with 1 < Te (apfu) < 3;
(3) potential 'ústalečite', with 3 < Te (apfu) < 4.

As remarked above, the structural information of arsenoústalečite and stibioústalečite leads to the end-member formulae $Cu_6Cu_6(As_2Te_2)Se_{12}S$ and $Cu_6Cu_6(Sb_2Te_2)Se_{12}S$, leaving the possibility for the existence of phases with a composition of $Cu_6Cu_6[(As/Sb)_2Te_2]Se_{12}Se$. Following Nickel and Grice (1998), these formulae should correspond to different mineral species, because "*at least one structural site* […]" is "*predominantly occupied by a different chemical component than that which occurs in the equivalent site in an existing mineral species*". However, the current nomenclature of the tetrahedrite group (Biagioni *et al.*, 2020) considers the dominance at the aggregate site S(1) + S(2), in order to avoid a further "proliferation" of mineral species.

Table 8. Comparison of Te-members of the tetrahedrite-group.

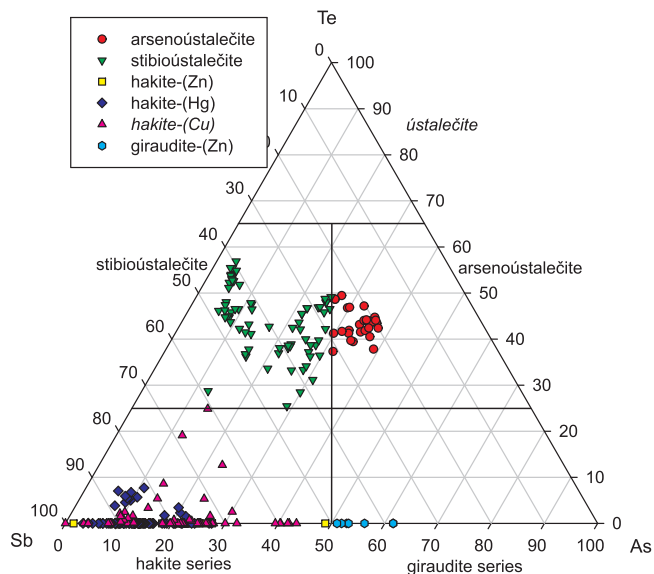|	Arsenoústalečite	Stibioústalečite	Arsenogoldfieldite	Stibiogoldfieldite
Ideal	$Cu_6Cu_6(As_2Te_2)Se_{13}$	$Cu_6Cu_6(Sb_2Te_2)Se_{13}$	$Cu_6Cu_6(As_2Te_2)S_{13}$	$Cu_6Cu_6(As_2Te_2)S_{13}$
$M(2)$	$(Cu_{5.81}Ag_{0.17})_{\Sigma 5.98}$	$(Cu_{5.69}Ag_{0.07})_{\Sigma 5.76}$	$Cu_{5.80}$	$(Cu_{6.09}Ag_{0.04})_{\Sigma 6.13}$
$M(1)$	$(Cu_{5.95}Fe_{0.02}Zn_{0.02}Hg_{0.01})_{\Sigma 6.00}$	$(Cu_{5.80}Zn_{0.13}Fe_{0.06}Hg_{0.01})_{\Sigma 6.00}$	$(Cu_{5.95}Zn_{0.03}Fe_{0.02})_{\Sigma 6.00}$	$(Cu_{5.96}Zn_{0.03}Fe_{0.01})_{\Sigma 6.00}$
$X(3)$	$(As_{1.40}Sb_{0.87}Te_{1.73})_{\Sigma 4.00}$	$(Sb_{1.82}As_{0.42}Te_{1.76})_{\Sigma 4.00}$	$(As_{1.44}Sb_{0.43}Bi_{0.13}Te_{2.00})_{\Sigma 4.00}$	$(Sb_{1.12}As_{0.63}Bi_{0.23}Te_{2.02})_{\Sigma 4.00}$
$S(1)+S(2)$	$(Se_{10.30}S_{2.32})_{\Sigma 12.61}$	$(Se_{9.52}S_{3.10})_{\Sigma 12.62}$	$S_{13.11}$	$(S_{12.99}Se_{0.11})_{\Sigma 13.10}$
a [Å]	10.6580(19)	10.6975(16)	10.2868(4)	10.3466(17)
V [Å³]	1210.7(6)	1224.2(5)	1088.53(13)	1107.6(5)
References	This work	This work	Sejkora *et al.* (2023a); unpublished data	Biagioni *et al.* (2022)

Actually, the different partitioning of Se and S between these two positions probably has a very important role, for instance avoiding too short $M(2)$–$S(2)$ bond distances (see, for instance, what happens in pošepnýite – Škácha et al., 2020), even if few structural data are currently available to achieve an accurate picture of the Se and S partitioning in tetrahedrite-group minerals. For this reason, the occurrence of significant S contents could be highlighted, using an adjectival modifier, like, for instance, S-bearing arsenoústalečite. The future identification of S-free members of the ústalečite series would allow for a better understanding of their crystal chemistry, also possibly improving the classification scheme of tetrahedrite-group minerals.

Genesis of members of the ústalečite series

De Medicis and Giasson (1971) and Hutabalian et al. (2023) examined the phase diagram of the Cu–Te–Se system at 340°C and 500°C, respectively, but did not find anything similar to 'ústalečite'. The absence of the synthetic analogue of ústalečite-like minerals in the experiments could have a double explanation.

On the one hand, it could suggest that arsenoústalečite and stibioústalečite formed at low T conditions. This would be confirmed by the presence of Cu selenides (athabascaite, berzelianite and umangite) in the association, which are formed at temperatures below 100–123°C (Harris et al., 1970; Simon and Essene, 1996; Škácha et al., 2017).

On the other hand, structural data collected on both species clearly indicated the dominance of S at the S(2) position. If this preferential partitioning is due to structural constraints [e.g. the necessity to avoid too short $M(2)$–$S(2)$ distances], it is possible that the absence of ústalečites in synthetic runs of the system Cu–Te–Se could be due to the absence of S that could play the same role of several minor chemical constituents observed in sulfosalts (e.g. Cl in dadsonite or O in meerschautite – Moëlo, 1979; Makovicky et al., 2006; Biagioni et al., 2016). Further studies will be useful to fully understand the actual compositional range of members of the ústalečite series.

Chemical variability of selenide members of the tetrahedrite group from Ústaleč

Figures 3 and 4 show the chemical composition for all studied samples of arsenoústalečite, stibioústalečite and other Se-dominant members of the tetrahedrite group from Ústaleč. Stibioústalečite is more common and it shows a wider range of As and Te contents; on the contrary, arsenoústalečite shows only a limited extent of Sb and Te contents, in the range 0.78–1.24 and 1.49–1.98 apfu, respectively. In other Se-dominant members of the tetrahedrite group, increased Te contents were determined only in the case of hakite-(Hg) and especially in the not-yet approved end-member 'hakite-(Cu)' (Fig. 3). The minor Ag contents for all studied grains of the ústalečite series are in the range 0.03–0.77 apfu and do not correlate with Sb, Te or S contents.
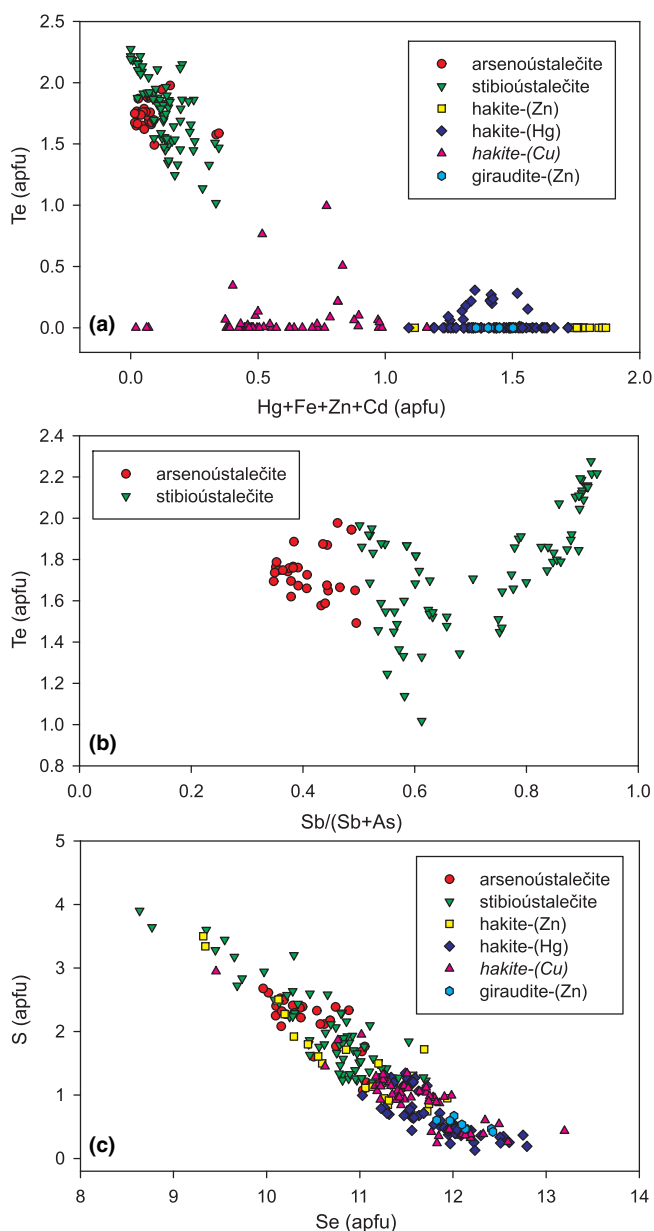
Figure 4. Compositional variation (in apfu) of Se-bearing tetrahedrite-group minerals from Ústaleč. **(a)** (Zn + Fe + Zn + Cd) vs. Te; **(b)** Sb/(Sb + As) vs. Te; and **(c)** Se vs. S.

Figure 3. Ternary Te–Sb–As diagram (at.%) for Se-dominant tetrahedrite-group minerals from Ústaleč.

The measured Me^{2+} contents (Me = Fe + Zn + Cd + Hg) in the minerals of the ústalečite series do not exceed 0.35 apfu (Fig. 4a). Their contents are in line with the substitution $^{M(1)}Me^{2+} + ^{X(3)}(Sb/As)^{3+} = ^{M(1)}Cu^+ + ^{X(3)}Te^{4+}$ reported for Te-rich members of the tetrahedrite group with Te contents up to 2 apfu (Biagioni *et al.*, 2020, 2022). Associated hakite-(Hg), hakite-(Zn) and giraudite-(Zn) show Me^{2+} contents in the range 1.09–1.87 apfu (Fig. 4a); members with Te < 1 apfu and Me^{2+} in the range 0.02–1.16 apfu (Fig. 4a) could correspond to the not-yet approved end-member 'hakite-(Cu)' with variable ratios of formally monovalent and divalent Cu. The determined Sb/(Sb + As) ratios *vs.* Te contents are plotted in Fig. 4b; the highest Te contents are observed in the As-poor members. The range of SeS_{-1} substitution is limited to 3.90 apfu S (Fig. 4c).

Conclusions

Arsenoústalečite is a new member of the tetrahedrite group and, along with stibioústalečite, forms a new series, namely the ústalečite series. The discovery of these species and the refinement of their crystal structures improve our knowledge of Te-dominant tetrahedrites and represents the first published refinements of selenide members of this sulfosalt group based on single-crystal X-ray diffraction data. Indeed, the only available refinement was that of hakite-(Hg) performed by Škácha *et al.* (2016) based on precession electron diffraction data (R = 24.4%). Moreover, the partitioning of Se and S between the two anion sites S(1) and S(2) opens some questions about the role of S in Se-dominant species. Indeed, even if Karup-Møller and Makovicky (1999) were able to synthesise the analogues of $Cu_{10}Zn_2Sb_4Se_{13}$ and $Cu_{10.2}Fe_{1.8}Sb_4Se_{13}$, in a S-free controlled environment, synthetic analogues of ústalečites were not obtained in the Cu–Te–Se system. If this is simply due to physical constraints (e.g. crystallisation T) or structural constraints (e.g. too short bond distances) is not clear and requires further study.

The quest for new tetrahedrite-group minerals promoted by the revision of their nomenclature (Biagioni *et al.*, 2020) resulted in a significant improvement in our knowledge about their crystal chemistry, through the collection of high-quality crystal chemical data. In this scenario, some open questions still remain to be solved but some findings, like that of arsenoústalečite, clearly confirm the fundamental role of the studies devoted to natural mineral assemblages to reveal novel crystal structures so far not obtained in laboratory experiments (e.g. De Medicis and Giasson, 1971; Hutabalian *et al.*, 2023; Bindi *et al.*, 2020).

References

Andreasen J.W., Makovicky E., Lebech B. and Karup-Møller S. (2008) The role of iron in tetrahedrite and tennantite determined by Rietveld refinement of neutron powder diffraction data. *Physics and Chemistry of Minerals*, **35**, 447–454.

Biagioni C., Moëlo Y., Orlandi P. and Stanley C.J. (2016) Lead-antimony sulfosalts from Tuscany (Italy). XVII. Meerschautite, $(Ag,Cu)_{5.5}Pb_{42.4}(Sb, As)_{45.1}S_{112}O_{0.8}$, a new expanded derivative of owyheeite from the Pollone mine, Valdicastello Carducci: occurrence and crystal structure. *Mineralogical Magazine*, **80**, 675–690.

Biagioni C., George L.G., Cook N.J., Makovicky E., Moëlo Y., Pasero M., Sejkora J., Stanley C.J., Welch M.D. and Bosi F. (2020) The tetrahedrite group: Nomenclature and classification. *American Mineralogist*, **105**, 109–122.

Biagioni C., Sejkora J., Musetti S., Makovicky E., Pagano R., Pasero M. and Dolníček Z. (2022) Stibiogoldfieldite, $Cu_{12}(Sb_2Te_2)S_{13}$, a new tetrahedrite-group mineral. *Mineralogical Magazine*, **86**, 168–175.

Bindi L., Nespolo M., Krivovichev S.V., Chapuis G. and Biagioni C. (2020) Producing highly complicated materials. Nature does it better. *Reports on Progress in Physics*, **83**, 106501.

Brese N.E. and O'Keeffe M. (1991) Bond-valence parameters for solids. *Acta Crystallographica*, **B47**, 192–197.

Christy A.G. (2015) Causes of anomalous mineralogical diversity in the Periodic Table. *Mineralogical Magazine*, **79**, 33–49.

Criddle A.J. and Stanley C.J. (1993) *Quantitative Data File for Ore Minerals*. Third edition. Chapman & Hall, London.

De Medicis R. and Giasson G. (1971) Le système Cu-Se-Te. *Comptes Rendus de l'Académie des Sciences – Series D*, **272**, 513–515.

Delgado J.M., Diaz de Delgado G., Quintero M. and Woolley J.C. (1992) The crystal structure of copper iron selenide, $CuFeSe_2$. *Materials Research Bulletin*, **27**, 367–373.

Flack H.D. (1983) On enantiomorph-polarity estimation. *Acta Crystallographica*, **A39**, 876–881.

Harris D.C., Cabri L.J. and Kaiman S. (1970) Athabascaite: A new copper selenide mineral from Martin Lake, Saskatchewan. *The Canadian Mineralogist*, **10**, 207–215.

Hutabalian Y., Chen Sw., and Gierlotka W. (2023) Phase equilibria of the Cu–Se–Te ternary system. *Journal of Phase Equilibria and Diffusion*, **44**, 181–199.

Kalbskopf R. (1974) Synthese und Kristallstruktur von $Cu_{12-x}Te_4S_{13}$, dem Tellur-Endglied der Fahlerze. *Tschermaks Mineralogische und Petrographische Mitteilungen*, **21**, 1–10.

Karup-Møller S. and Makovicky E. (1999) Exploratory studies of element substitutions in synthetic tetrahedrite. Part II. Selenium and tellurium as anions in Zn-Fe tetrahedrites. *Neues Jahrbuch für Mineralogie, Monatshefte*, **1999**, 385–399.

Kato A. and Sakurai K. (1970) Re-definition of goldfieldite $Cu_{12}(Te,As,Sb)_4S_{13}$. *Journal of the Mineralogical Society of Japan*, 10, 122 [in Japanese].

Kraus W. and Nolze G. (1996) POWDER CELL − a program for the representation and manipulation of crystal structures and calculation of the resulting X-ray powder patterns. *Journal of Applied Crystallography*, **29**, 301–303.

Litochleb J., Šrein V., Novická Z. and Šreinová B. (1999) Selenides from the uranium deposit Ústaleč (SW Bohemia). *Bulletin mineralogicko-petrologického oddělení Národního muzea v Praze*, 7, 98–108 [in Czech].

Makovicky E. and Karup-Møller S. (2017) Exploratory studies of substitutions in the tetrahedrite/tennantite goldfieldite solid solution. *The Canadian Mineralogist*, **55**, 233–244.

Makovicky E., Karanović L., Poleti D., Balić-Žunić T. and Paar W.H. (2005) Crystal structure of copper-rich unsubstituted tennantite, $Cu_{12.5}As_4S_{13}$. *The Canadian Mineralogist*, **43**, 679–688.

Makovicky E., Topa D. and Mumme W.G. (2006) The crystal structure of dadsonite. *The Canadian Mineralogist*, **44**, 1499–1512.

Moëlo Y. (1979) Quaternary compounds in the system Pb–Sb–S–Cl: dadsonite and synthetic phases. *The Canadian Mineralogist*, **17**, 595–600.

Moëlo Y., Makovicky E., Mozgova N.N., Jambor J.L., Cook N., Pring A., Paar W.H., Nickel E.H., Graeser S., Karup-Møller S., Balić-Žunić T., Mumme W.G., Vurro F., Topa D., Bindi L., Bente K. and Shimizu M. (2008) Sulfosalt systematics: a review. Report of the sulfosalt sub-committee of the IMA Commission on Ore Mineralogy. *European Journal of Mineralogy*, **20**, 7–46.

Nickel E.H. and Grice J.D. (1998) The IMA Commission on New Minerals and Mineral Names: procedures and guidelines on mineral nomenclature, 1998. *The Canadian Mineralogist*, **36**, 913–926.

Noviello S.P. (1989) *Paragenesis, fluid inclusion study, microprobe analysis and geochemistry of the gold-telluride mineralizing fluids at the Wild Dog Prospect, PNG*. B.Sc. (Hon.) thesis, Monash University, Clayton, Victoria. Australia.

Pasero M. (2023) The New IMA List of Minerals. International Mineralogical Association. Commission on new minerals, nomenclature and classification (IMA-CNMNC). http://cnmnc.units.it/ [Accessed June 2023].

Pohl D., Ließmann W. and Okrugin V.M. (1996) Rietveld analysis of selenium-bearing goldfieldites. *Neues Jahrbuch für Mineralogie, Monatshefte*, **1996**, 1–8.

Pouchou J.L., and Pichoir F. (1985) "PAP" ($\varphi\rho Z$) procedure for improved quantitative microanalysis. Pp. 104–106 in: *Microbeam Analysis* (J.T. Armstrong, editor). San Francisco Press, San Francisco.

Ransome F.L. (1909) *Geology and Ore Deposits of Goldfield, Nevada*. U.S. Geological Survey, Professional Papers, 66.

Sejkora J., Plášil J. and Makovicky E. (2022) Stibioústalečite, $Cu_6Cu_6(Sb_2Te_2)Se_{13}$, the first Te–Se member of tetrahedrite group, from the Ústaleč, Czech Republic. *Journal of Geosciences*, **67**, 289–297.

Sejkora J., Biagioni C., Dolníček Z. and Voudouris P. (2023a) Arsenogoldfieldite, IMA 2022-084. CNMNC Newsletter 70; *Mineralogical Magazine*, **87**, https://doi.org/10.1180/mgm.2022.135.

Sejkora J., Mauro D. and Biagioni C. (2023b) Single-crystal structure refinement of bukovite, $(Cu_3Fe)_{\Sigma4}Tl_2Se_4$. *Journal of Geosciences*, **68**, 179–184.

Sharwood W.J. (1907) Gold tellurides. *Mining and Scientific Press*, **94**, 731–732.

Sheldrick G.M. (2015) Crystal structure refinement with SHELXL. *Acta Crystallographica*, **C71**, 3–8.

Simon G. and Essene E.J. (1996) Phase relations among selenides, sulfides, tellurides, and oxides. I. Thermodynamic properties and calculated equilibria. *Economic Geology*, **91**, 1183–1208.

Škácha P., Sejkora J., Palatinus L., Makovicky E., Plášil J., Macek I. and Goliáš V. (2016) Hakite from Příbram, Czech Republic: compositional variability, crystal structure and the role in Se mineralization. *Mineralogical Magazine*, **80**, 1115–1128.

Škácha P., Sejkora J. and Plášil J. (2017) Selenide mineralization in the Příbram uranium and base-metal district (Czech Republic). *Minerals*, **7**, 91.

Škácha P., Sejkora J., Plášil J. and Makovicky E. (2020) Pošepnýite, a new Hg-rich member of the tetrahedrite group from Příbram, Czech Republic. *Journal of Geosciences*, **65**, 173–186.

Spiridonov E.M. and Okrugin V.M. (1985) Selenium goldfieldite, a new fahlore variety. *Doklady Akademii Nauk SSSR*, **280**, 474–478.

Spiridonov E.M., Ivanova Yu.N. and Yapaskurt V.O. (2014) Selenium-bearing goldfieldite and fischesserite $AuAg_3Se_2$ − petzite $AuAg_3Te_2$ solid solutions in ores from the Ozernovskoe volcanogenic deposit (Kamchatka). *Doklady Earth Science*, **458**, 1139–1142.

Thompson R.M. (1946) Goldfieldite-tellurian tetrahedrite. *University of Toronto Studies, Geological Series*, **50**, 77–78.

Trudu A.G. and Knittel U. (1998) Crystallography, mineral chemistry and chemical nomenclature of goldfieldite, the tellurian member of the tetrahedrite solid-solution series. *The Canadian Mineralogist*, **36**, 1115–1137.

Wedepohl K.H. (1995) The composition of the continental crust. *Geochimica et Cosmochimica Acta*, **59**, 1217–1232.

Welch M.D., Stanley C.J., Spratt J. and Mills S.J. (2018) Rozhdestvenskayaite $Ag_{10}Zn_2Sb_4S_{13}$ and argentotetrahedrite $Ag_6Cu_4(Fe^{2+},Zn)_2Sb_4S_{13}$: two Ag-dominant members of the tetrahedrite group. *European Journal of Mineralogy*, **30**, 1163–1172.

Wilson A.J.C. (editor) (1992) *International Tables for Crystallography Volume C: Mathematical, Physical and Chemical Tables*. Kluwer Academic Publishers, Dordrecht, The Netherlands.